Confined Quasiparticle Dynamics in Long-Range Interacting Quantum Spin Chains

Fangli Liu,[1] Rex Lundgren,[1] Paraj Titum,[1,2] Guido Pagano,[1] Jiehang Zhang,[1]
Christopher Monroe,[1,2] and Alexey V. Gorshkov[1,2]
[1]*Joint Quantum Institute, NIST/University of Maryland, College Park, Maryland 20742, USA*
[2]*Joint Center for Quantum Information and Computer Science, NIST/University of Maryland, College Park, Maryland 20742, USA*

(Received 17 October 2018; revised manuscript received 31 January 2019; published 16 April 2019)

We study the quasiparticle excitation and quench dynamics of the one-dimensional transverse-field Ising model with power-law ($1/r^{\alpha}$) interactions. We find that long-range interactions give rise to a confining potential, which couples pairs of domain walls (kinks) into bound quasiparticles, analogous to mesonic states in high-energy physics. We show that these quasiparticles have signatures in the dynamics of order parameters following a global quench, and the Fourier spectrum of these order parameters can be exploited as a direct probe of the masses of the confined quasiparticles. We introduce a two-kink model to qualitatively explain the phenomenon of long-range-interaction-induced confinement and to quantitatively predict the masses of the bound quasiparticles. Furthermore, we illustrate that these quasiparticle states can lead to slow thermalization of one-point observables for certain initial states. Our work is readily applicable to current trapped-ion experiments.

DOI: 10.1103/PhysRevLett.122.150601

Long-range interacting quantum systems occur naturally in numerous quantum simulators [1–10]. A paradigmatic model considers interactions decaying with distance r as a power law $1/r^{\alpha}$. This describes the interaction term in trapped-ion spin systems [3,11–15], polar molecules [16–19], magnetic atoms [5,20,21], and Rydberg atoms [1,2,22,23]. One remarkable consequence of long-range interactions is the breakdown of locality, where quantum information bounded by linear "light cones" in short-range interacting systems [24] can propagate superballistically or even instantaneously [25–31]. The nonlocal propagation of quantum correlations in 1D systems has been observed in trapped-ion experiments [12,13]. Moreover, 1D long-range interacting quantum systems can host novel physics that is absent in their short-range counterparts, such as continuous symmetry breaking [32,33].

Recently, it has been shown that confinement—which has origins in high-energy physics—has dramatic signatures in the quantum quench dynamics of short-range interacting spin chains [34]. Owing to confinement, quarks cannot be directly observed in nature as they form mesons and baryons due to strong interactions [35,36]. An archetypal model with analogous confinement effects in quantum many-body systems is the 1D short-range interacting Ising model with both transverse and longitudinal fields [37–42]. For a vanishing longitudinal field, domain-wall quasiparticles propagate freely and map out light-cone spreading of quantum information [41–44]. As first proposed by McCoy and Wu [45,46] (see also Ref. [47]), a nonzero longitudinal field induces an attractive linear potential between two domain walls and confines them into mesonic quasiparticles. Recently, Kormos *et al.* investigated global quenches in this system and showed that the nonequilibrium dynamics can be used to probe the confined quasiparticle excitations [34].

In this work, we study the nonequilibrium dynamics of the long-range interacting transverse-field Ising model without a longitudinal field after a global quantum quench. We find that long-range interactions introduce an effective attractive force between a pair of domain walls, thus, confining them into a bound state analogous to the meson in high-energy physics. We calculate time-dependent order parameters and connected correlation functions, both of which feature clear signatures of confined quasiparticle excitations [41,42]. The masses of these bound quasiparticles—the energy gaps relative to the ground state—can be directly extracted from the Fourier spectrum of time-dependent order parameters [34,41,42]. We introduce a two-kink model to explicitly show that the confining potential comes from long-range interactions. This effective model also gives good predictions for the quasiparticles' masses and their dispersion relations. Furthermore, we study the effect of confined quasiparticles on the thermalization of different initial states. We find that for certain initial states, one-point observables exhibit slow thermalization [41,42,48,49], which might help protect ordered phases in the prethermal region [50–52].

We note that our study is in agreement with the general mechanism of global quantum quenches, first formulated in Refs. [41,42,44] for short-range interacting systems, and demonstrates that the general theory developed in Refs. [41,42,44] holds for systems with long-range interactions. Our work is well within the reach of current trapped-ion experiments [15] and other atomic, molecular, and optical (AMO) experimental platforms [1,9,53].

The model.—Let us consider a quantum spin chain with long-range interactions described by the following Hamiltonian,

$$H = -\sum_{i<j}^{L} \frac{J}{r_{ij}^{\alpha}} \sigma_i^z \sigma_j^z - B \sum_{i=1}^{L} \sigma_i^x, \tag{1}$$

where σ_i^{μ} are the Pauli matrices on site i, L is the system size, r_{ij} is the distance between sites i and j (nearest-neighbor spacing is set to 1), J sets the overall energy scale (set to 1), B is a global transverse field, and α describes the power-law decay of long-range interactions. In this work, we consider periodic boundary conditions unless otherwise specified [$r_{ij} = \min(|i-j|, L-|i-j|)$].

In the nearest-neighbor interacting limit ($\alpha \to \infty$), H is exactly solvable via a Jordan-Wigner mapping to spinless fermions. It exhibits a phase transition at $B = 1$, which separates the ferromagnetic and paramagnetic regions [54]. The phase transition persists for long-range interactions, while the critical value of B increases [55–58]. In trapped-ion experiments, the range of the exponent can be tuned within $0 \leq \alpha \leq 3$ by changing the detuning of the applied optical fields from phonon sidebands. We restrict the numerics to $\alpha > 1$ in order to ensure a well-behaved thermodynamic limit (the case of $\alpha \in [0, 1]$ will be discussed later). Several experiments have investigated the real-time dynamics of the above model (or closely related models), including dynamical phase transitions [15,59], the nonlocal propagation of correlations [12,13], time crystals [50], and many-body localization [14].

Quench dynamics.—We first study the quench dynamics of the above model. We focus on an initial state with all spins polarized in the z direction $|\Psi_0\rangle = |\ldots\uparrow\uparrow\uparrow\ldots\rangle$, which is easily preparable in trapped-ion experiments [15]. The system is allowed to evolve under the Hamiltonian (1). This is equivalent to a global quantum quench from zero to finite B [15,41,42]. In order to explore the physics of domain walls, we focus on quantum quenches within the ferromagnetic phase [43,60]. We mention that similar features persist when the initial state is chosen as the ground state of Eq. (1) with finite B in the ferromagnetic region.

We use the Krylov-space method to simulate the quench dynamics of our system [61,62]. Figures 1(a)–1(c) show the equal-time connected correlation functions $\langle \sigma_j^z(t)\sigma_k^z(t)\rangle_c = \langle \sigma_j^z(t)\sigma_k^z(t)\rangle - \langle \sigma_j^z(t)\rangle\langle \sigma_k^z(t)\rangle$ after the sudden quench (k indicates the central lattice site). In the short-range interacting limit [Fig. 1(a)], we recover the exactly solvable case, where correlations spread with a velocity ($4B$) equal to twice the maximal speed of free domain walls [34,43,44]. Increasing the Ising interaction range (decreasing α) strongly suppresses the magnitude of $\langle \sigma_j^z(t)\sigma_k^z(t)\rangle_c$, as shown in Figs. 1(b) and 1(c). One can also see the oscillatory behavior of correlations [Figs. 1(b) and 1(c)], similar to that of Ref. [34]. However, we emphasize that the light-cone spreading of correlations is always present

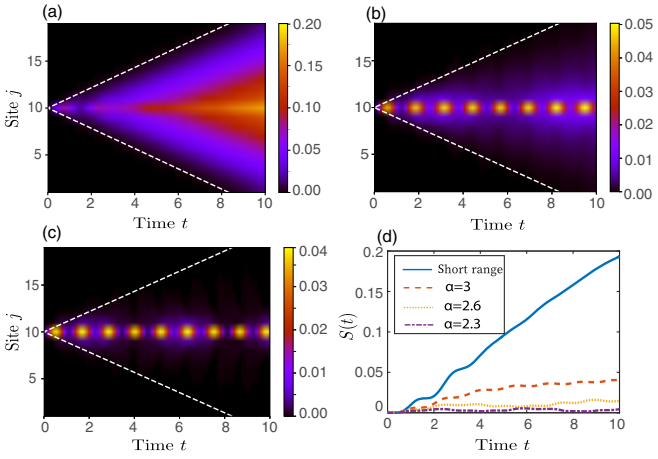

FIG. 1. (a)–(c) $\langle \sigma_j^z\sigma_k^z\rangle_c$ and (d) $S_A(t)$ versus t after a quantum quench with initial state $|\Psi_0\rangle$. $L = 19$, $k = 10$, and $B = 0.27$. (a) Short-range interacting case ($\alpha \to \infty$), (b) $\alpha = 2.6$, (c) $\alpha = 2.3$. The dashed white lines illustrate the maximal velocity $4B$ of freely propagating domain walls in the short-range interacting case [34]. (d) $S_A(t)$ for various α.

[34,44], though it may have a different velocity depending on the quasiparticles in the system [44]. The actual extent of the light cone becomes clearer by displaying the correlation functions presented in Figs. 1(b) and 1(c) on a different intensity scale (see Supplemental Material [63]). This result is in agreement with the general mechanism of global quantum quenches first derived in Ref. [44].

The propagating quasiparticles produced by the quench map out the light-cone spreading of correlations [44,63] and lead to the growth of entanglement entropy [34]. Figure 1(d) shows the growth of entanglement entropy, $S_A(t) = -\mathrm{Tr}\{\rho_A(t)\ln[\rho_A(t)]\}$, where $\rho_A(t)$ is the reduced density matrix of one-half of the chain for various α. As one can see, the entanglement entropy growth for smaller α is much slower than the short-range case (linear growth) [28]. This is because the propagating quasiparticles have smaller velocities for longer-range interactions [63].

We plot time-dependent order parameters $\langle \sigma^z(t)\rangle = (1/L)\sum_i \langle \sigma_i^z(t)\rangle$ in Figs. 2(a) and 2(b) [64]. Different from the rapid exponential decay of the magnetization for the short-range case, $\langle \sigma^z(t)\rangle$ exhibits periodic oscillations with almost no decay [41,42,65–67] in the time window shown here. We emphasize that the qualitative change in dynamics is caused by the long-range interactions, not by an additional longitudinal field as in the short-range interacting case [34]. The Fourier spectrum of $\langle \sigma^z(t)\rangle$ illustrates that the oscillations are associated with multiple frequencies [Figs. 2(c) and 2(d)]. As we will see, these frequencies coincide with the masses (and their differences) of quasiparticles [41,42].

Two-kink model and bound states.—To understand the quasiparticles in our system, we use a two-kink model to perturbatively study the low-energy excitations of Eq. (1). The two-kink model has been used to phenomenologically

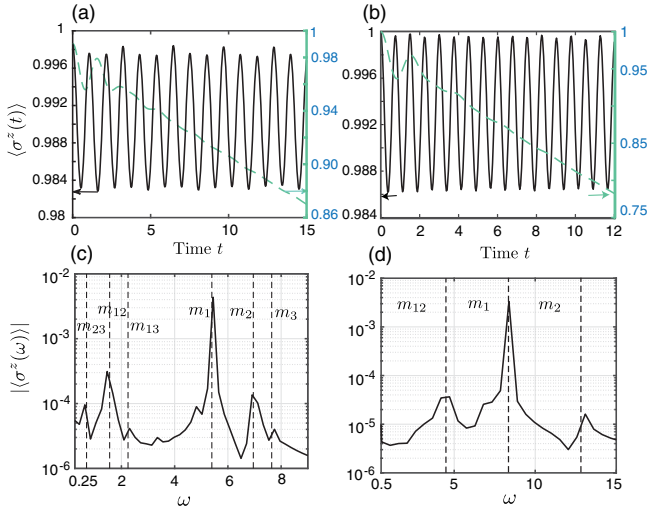

FIG. 2. (a),(b) $\langle\sigma^z(t)\rangle$ (black line) versus time after quenching to (a) $\alpha = 2.3$, $B = 0.27$, (b) $\alpha = 1.4$, $B = 0.35$ for $L = 20$. The dashed green lines show $\langle\sigma^z(t)\rangle$ for the short-range model (same B). (c),(d) Fourier spectrum of $\langle\sigma^z(t)\rangle$ for the long-range case in (a) and (b), respectively. The largest time for the Fourier transform is $t = 30$ and 12 for (c) and (d), respectively. The parameters in (b),(d) are accessible in current trapped-ion experiments [15]. The dashed lines show the mesonic masses (m_i) and their differences ($m_{ij} \equiv m_j - m_i$) calculated using the two-kink model.

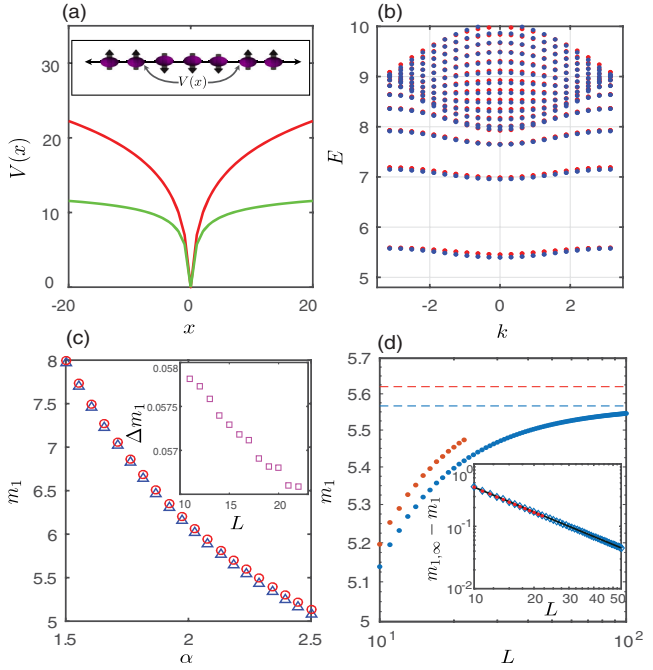

FIG. 3. (a) Potential energy as a function of distance x between the two domain walls ($n = |x|$). Red line, $\alpha = 1.9$; green line, $\alpha = 2.3$. Inset: Typical spin configuration of two-domain-wall states. (b)–(d) Comparison of two-kink model (blue) and ED results (red). (b) Energy spectrum. Parameters: $\alpha = 2.3$, $B = 0.27$, $L = 20$. (c) m_1 versus α with parameters $B = 0.27$ and $L = 22$. Inset: Difference of m_1 between the two methods Δm_1 versus L. (d) m_1 versus L [same parameters as (b)]. The dashed lines are $m_{1,\infty}$. The inset shows $m_{1,\infty} - m_1$ versus system size. The black line shows the fitting of the two-kink model's data to $(1/L)^\beta$, with $\beta = 1.315$. ED data have similar scaling with $\beta = 1.34$. $m_{1,\infty}$ is chosen as 5.56 (5.62) for the two-kink model (ED).

study excitations in short-range interacting quasi-1D compounds [37,68]. The idea is to restrict the Hilbert space to two-domain-wall states [see inset of Fig. 3(a)], where regions of different magnetization are separated by the two domain walls. The projected model is expected to work well when B is much smaller than J [34].

The Hilbert space of the projected model is spanned by states of n down spins (clustered together) represented as $|j,n\rangle = |\ldots\uparrow\uparrow\downarrow_j\downarrow\ldots\downarrow\downarrow_{(j+n-1)}\uparrow\uparrow\ldots\rangle$, where j is the starting position of the cluster. The projected Hamiltonian $\mathcal{H} = \mathcal{P}H\mathcal{P}$ ($\mathcal{P}$ denotes the projection operator to the two-domain-wall subspace) acts on $|j,n\rangle$ as follows:

$$\mathcal{H}|j,n\rangle = V(n)|j,n\rangle - B[|j,n+1\rangle + |j,n-1\rangle + |j+1,n+1\rangle + |j-1,n+1\rangle]. \quad (2)$$

Here, we have defined the potential energy as $V(n) = \langle j,n|\mathcal{H}|j,n\rangle - \langle\Psi_0|\mathcal{H}|\Psi_0\rangle$. Utilizing translational invariance, we transform the two-domain-wall state into momentum basis $|k,n\rangle = (1/\sqrt{L})\sum_{j=1}^{L}\exp(-ikj - ikn/2)|j,n\rangle$, which gives

$$\mathcal{H} = \sum_{k,n} V(n)|k,n\rangle\langle k,n| - 2B\cos\frac{k}{2}|k,n\rangle\langle k,n+1| - 2B\cos\frac{k}{2}|k,n\rangle\langle k,n-1|. \quad (3)$$

For $L \to \infty$, the potential energy of a two-domain-wall spin configuration is

$$V(n) = 4n\zeta(\alpha)J - 4J\sum_{1\le l<n}\sum_{1\le r\le l}\frac{1}{r^\alpha}, \quad (4)$$

where $\zeta(\alpha) = \sum_{z=1}^{\infty}(1/z^\alpha)$ denotes the Riemann zeta function. As plotted in Fig. 3(a), $V(n)$ *increases* with the distance between domain walls. For the short-range model studied in Ref. [34], the confining potential is due to an additional on-site longitudinal magnetic field. In our case, the confining potential is intrinsically generated by the long-range interactions.

The picture now becomes clear: The long-range Ising interaction gives rise to an effective potential, which *increases* with separation between the two domain walls, while the transverse magnetic field acts as kinetic energy for domain walls (changing the size of the cluster). Therefore, a pair of domain walls, each of which is a free quasiparticle in the short-range limit, becomes bounded together when α decreases. Note that $V(n)$ has an upper bound when $\alpha > 2$, as illustrated in Fig. 3(a) (see Supplemental Material [63]). This indicates that the lower part of the energy spectrum is composed of domain-wall bound states, while above some

energy threshold, we have a continuum of states [Fig. 3(b)]. For $\alpha \leq 2$, however, all excitations within the two-kink model are bound quasiparticles, as the confining potential $V(n)$ becomes unbounded when $n \to \infty$ [63]. This is in contrast with finite-range interacting models, where the potential becomes *flat* for n greater than the interaction range. In other words, for finite-range interacting systems, two domain walls will behave like freely propagating particles if the domain size of the initial state exceeds the interaction range.

Figure 3(b) shows the energy spectrum calculated by the two-kink model (blue dots) and exact diagonalization (ED) of the full Hamiltonian (red dots). The energy spectrum agrees well for the two methods, demonstrating that low-energy excitations are dominated by two-domain-wall states. The bound states' masses [69] and dispersion relations can be simply read out from the energy spectrum. Moreover, the Fourier frequencies of $\langle \sigma^z(t) \rangle$ [Figs. 2(c) and 2(d)] coincide, to high accuracy, with the masses of the bound states (and their differences) calculated using the two-kink model [41,42]. This demonstrates that the quench dynamics of the long-range interacting model is indeed dominated by confined quasiparticles.

We compare the smallest quasiparticle mass m_1 as a function of α calculated using the two-kink model and ED [Fig. 3(c)]. For a large range of α, we see excellent agreement between the two methods, and the numerical difference does not increase for larger L [inset of Fig. 3(c)]. The masses increase with L as longer chains have more interaction terms [63]. However, $V(n)$ is finite (for finite n) in the thermodynamic limit, since the Riemann zeta function converges for $\alpha > 1$ [70]. This leads to finite masses, even for an infinite system for $\alpha > 1$ (see Supplemental Material [63]). As shown in Fig. 3(d), the mass calculated from the two-kink model indeed exhibits convergence in the thermodynamic limit. For the two-kink model, the difference between m_1 and its thermodynamic value $m_{1,\infty}$ scales as $(1/L)^{\beta}$, with $\beta \approx \alpha - 1$ [63], as shown in the inset. While we cannot verify convergence using ED, we do observe similar scaling of m_1 [inset of Fig. 3(d)]. For $0 \leq \alpha \leq 1$, $V(n)$ becomes infinite, even for finite n, and thus, the quasiparticles have infinite energy (as the Riemann zeta function diverges for $0 \leq \alpha \leq 1$ [70]), consistent with the results of Ref. [71].

Strong and weak thermalization.—For the quenches we have considered, both the order parameter decay and entanglement growth are slow (Fig. 1). This motivates us to study thermalization in our long-range model. Previous studies of the short-range Ising model have observed rapid (strong) or slow (weak) thermalization of one-point functions for different initial states [41,42,48,49,72–75]. As first shown in Ref. [41], undamped oscillations (weak thermalization) of a one-point observable occur within an intermediate time window when the matrix elements between the initial state and the quasiparticle state of the quench operator and of the observable are both nonzero [41,42]. Rapid decay occurs when this condition is not satisfied. Numerical results consistent with this finding have been observed [34,42,48,49,74]. Here, we illustrate that these two distinct behaviors also occur in the long-range Ising model and that slow thermalization can arise when the quasiparticles are the result of confinement [34,42,74].

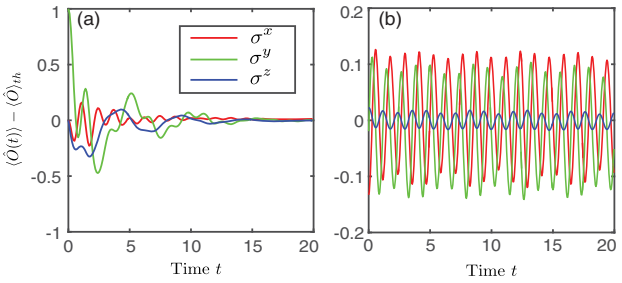

FIG. 4. Strong (a) and weak (b) thermalization for different initial states. (a) $\langle \sigma^{\mu}(t) \rangle - \langle \sigma^{\mu} \rangle_{\text{th}}$ for initial state $|Y_+\rangle$. (b) Same as (a) but for initial state $|Z_+\rangle$. Parameters: $\alpha = 2.3$, $B = 0.37$, $L = 20$.

In order to see this, we consider the time evolution of two different initial states (with the same quenched Hamiltonian): $|Z_+\rangle = \prod_j |\uparrow_j\rangle$ (the same state considered before) and $|Y_+\rangle = \prod_j (1/\sqrt{2})(|\uparrow_j\rangle + i|\downarrow_j\rangle)$ [48]. For $|Z_+\rangle$, the quenched operator has the same parity as the two-kink bound state, and thus, the matrix elements mentioned above have nonzero values [41,42]. We therefore expect slow dynamics with oscillations due to the bound quasiparticles [41,42]. On the other hand, $|Y_+\rangle$ does not satisfy this condition, which suggests rapid thermalization.

We calculate the difference between the time-dependent expectation value of single-body observables $\langle \sigma^{\mu}(t) \rangle$ and their thermal expectation value $\langle \sigma^{\mu} \rangle_{\text{th}} = \text{tr}(e^{-\beta_\Psi H} \sigma^{\mu})/\text{tr}(e^{-\beta_\Psi H})$, where the temperature $1/\beta_\Psi$ is determined by [76]

$$\frac{\langle \Psi | H | \Psi \rangle}{\langle \Psi | \Psi \rangle} = \frac{\text{tr}(H e^{-\beta_\Psi H})}{\text{tr}(e^{-\beta_\Psi H})}. \tag{5}$$

Here, $|\Psi\rangle$ denotes the initial state. As illustrated in Fig. 4(a), for $|Y_+\rangle$, all single-body observables converge to $\langle \sigma^{\mu} \rangle_{\text{th}}$ rapidly, indicating strong thermalization, as expected. For $|Z_+\rangle$, we instead observe strong oscillatory behavior [41,42], with Fourier frequencies consistent with the masses of the bound quasiparticles, around $\langle \sigma^{\mu} \rangle_{\text{th}}$ [Fig. 4(b)]. Within the time window shown, we observe almost no decay of these observables, indicating much slower thermalization compared to $|Y_+\rangle$ [48,49].

Conclusions and outlook.—We have found that the low-energy excitations of the long-range transverse-field Ising model are confined domain walls. These bound quasiparticles, which arise due to long-range interactions, have clear signatures in the quench dynamics of the system [34,41,42]. Furthermore, our work has shown that general quantum mechanisms of quench dynamics developed for short-range interacting systems [41,42,44] hold for long-range

interacting systems. These results can be readily investigated in trapped-ion experiments [15] and other AMO systems with long-range interactions [1,9,53]. The slow thermalization of one-point functions induced by long-range interactions has potential applications for stabilizing nonequilibrium phases of matter, such as time crystals [50–52] and Floquet symmetry-protected topological phases of matter [77–81]. Finally, it would be interesting to study the effects of long-range interactions on quench dynamics of q-state Potts models, which admit mesonic as well as baryonic excitations [82–85].

We are grateful to F. Verstraete, P. Calabrese, A. Bapat, J. Garrison, S. K. Chu, C. Flower, and S. Whitsitt for useful discussions. F. L., R. L., and A. V. G. acknowledge support by ARO, NSF Ideas Lab on Quantum Computing, the DOE ASCR Quantum Testbed Pathfinder program, DOE BES Materials and Chemical Sciences Research for Quantum Information Science program, ARL Center for Distributed Quantum Information, NSF PFC at Joint Quantum Institute, and ARO MURI. R. L. and P. T. were supported by NIST NRC Research Postdoctoral Associateships. G. P., J. Z., and C. M. are supported by the ARO and AFOSR Atomic and Molecular Physics Programs, the AFOSR MURI on Quantum Measurement and Verification, the IARPA LogiQ program, and the NSF Physics Frontier Center at JQI. This research was supported in part by the National Science Foundation under Grant No. NSF PHY-1748958.

[1] M. Saffman, T. G. Walker, and K. Mølmer, Quantum information with Rydberg atoms, Rev. Mod. Phys. **82**, 2313 (2010).
[2] P. Schauß, M. Cheneau, M. Endres, T. Fukuhara, S. Hild, A. Omran, T. Pohl, C. Gross, S. Kuhr, and I. Bloch, Observation of spatially ordered structures in a two-dimensional Rydberg gas, Nature (London) **491**, 87 (2012).
[3] R. Islam, C. Senko, W. C. Campbell, S. Korenblit, J. Smith, A. Lee, E. E. Edwards, C.-C. J. Wang, J. K. Freericks, and C. Monroe, Emergence and frustration of magnetism with variable-range interactions in a quantum simulator, Science **340**, 583 (2013).
[4] F. Dolde, I. Jakobi, B. Naydenov, N. Zhao, S. Pezzagna, C. Trautmann, J. Meijer, P. Neumann, F. Jelezko, and J. Wrachtrup, Room-temperature entanglement between single defect spins in diamond, Nat. Phys. **9**, 139 (2013).
[5] M. Lu, N. Q. Burdick, and B. L. Lev, Quantum Degenerate Dipolar Fermi Gas, Phys. Rev. Lett. **108**, 215301 (2012).
[6] L. Childress, M. V. G. Dutt, J. M. Taylor, A. S. Zibrov, F. Jelezko, J. Wrachtrup, P. R. Hemmer, and M. D. Lukin, Coherent dynamics of coupled electron and nuclear spin qubits in diamond, Science **314**, 281 (2006).
[7] J. R. Weber, W. F. Koehl, J. B. Varley, A. Janotti, B. B. Buckley, C. G. Van de Walle, and D. D. Awschalom, Quantum computing with defects, Proc. Natl. Acad. Sci. U.S.A. **107**, 8513 (2010).
[8] S. Gopalakrishnan, B. L. Lev, and P. M. Goldbart, Frustration and Glassiness in Spin Models with Cavity-Mediated Interactions, Phys. Rev. Lett. **107**, 277201 (2011).
[9] J. S. Douglas, H. Habibian, C.-L. Hung, A. V. Gorshkov, H. J. Kimble, and D. E. Chang, Quantum many-body models with cold atoms coupled to photonic crystals, Nat. Photonics **9**, 326 (2015).
[10] C.-L. Hung, A. González-Tudela, J. I. Cirac, and H. J. Kimble, Quantum spin dynamics with pairwise-tunable, long-range interactions, Proc. Natl. Acad. Sci. U.S.A. **113**, E4946 (2016).
[11] J. W. Britton, B. C. Sawyer, A. C. Keith, C.-C. J. Wang, J. K. Freericks, H. Uys, M. J. Biercuk, and J. J. Bollinger, Engineered two-dimensional Ising interactions in a trapped-ion quantum simulator with hundreds of spins, Nature (London) **484**, 489 (2012).
[12] P. Richerme, Z.-X. Gong, A. Lee, C. Senko, J. Smith, M. Foss-Feig, S. Michalakis, A. V. Gorshkov, and C. Monroe, Non-local propagation of correlations in quantum systems with long-range interactions, Nature (London) **511**, 198 (2014).
[13] P. Jurcevic, B. P. Lanyon, P. Hauke, C. Hempel, P. Zoller, R. Blatt, and C. F. Roos, Quasiparticle engineering and entanglement propagation in a quantum many-body system, Nature (London) **511**, 202 (2014).
[14] J. Smith, A. Lee, P. Richerme, B. Neyenhuis, P. W. Hess, P. Hauke, M. Heyl, D. A. Huse, and C. Monroe, Many-body localization in a quantum simulator with programmable random disorder, Nat. Phys. **12**, 907 (2016).
[15] J. Zhang, G. Pagano, P. W. Hess, A. Kyprianidis, P. Becker, H. Kaplan, A. V. Gorshkov, Z.-X. Gong, and C. Monroe, Observation of a many-body dynamical phase transition with a 53-qubit quantum simulator, Nature (London) **551**, 601 (2017).
[16] K.-K. Ni, S. Ospelkaus, M. H. G. de Miranda, A. Pe'er, B. Neyenhuis, J. J. Zirbel, S. Kotochigova, P. S. Julienne, D. S. Jin, and J. Ye, A high phase-space-density gas of polar molecules, Science **322**, 231 (2008).
[17] K.-K. Ni, S. Ospelkaus, D. Wang, G. Quéméner, B. Neyenhuis, M. H. G. de Miranda, J. L. Bohn, J. Ye, and D. S. Jin, Dipolar collisions of polar molecules in the quantum regime, Nature (London) **464**, 1324 (2010).
[18] A. Chotia, B. Neyenhuis, S. A. Moses, B. Yan, J. P. Covey, M. Foss-Feig, A. M. Rey, D. S. Jin, and J. Ye, Long-Lived Dipolar Molecules and Feshbach Molecules in a 3D Optical Lattice, Phys. Rev. Lett. **108**, 080405 (2012).
[19] P. K. Molony, P. D. Gregory, Z. Ji, B. Lu, M. P. Köppinger, C. R. Le Sueur, C. L. Blackley, J. M. Hutson, and S. L. Cornish, Creation of Ultracold $^{87}Rb^{133}Cs$ Molecules in the Rovibrational Ground State, Phys. Rev. Lett. **113**, 255301 (2014).
[20] K. Aikawa, A. Frisch, M. Mark, S. Baier, A. Rietzler, R. Grimm, and F. Ferlaino, Bose-Einstein Condensation of Erbium, Phys. Rev. Lett. **108**, 210401 (2012).
[21] G. Balasubramanian, P. Neumann, D. Twitchen, M. Markham, R. Kolesov, N. Mizuochi, J. Isoya, J. Achard, J. Beck, J. Tissler, V. Jacques, P. R. Hemmer, F. Jelezko, and J. Wrachtrup, Ultralong spin coherence time in isotopically engineered diamond, Nat. Mater. **8**, 383 (2009).

[22] L. Béguin, A. Vernier, R. Chicireanu, T. Lahaye, and A. Browaeys, Direct Measurement of the van der Waals Interaction between Two Rydberg Atoms, Phys. Rev. Lett. **110**, 263201 (2013).

[23] Y. O. Dudin and A. Kuzmich, Strongly Interacting Rydberg Excitations of a Cold Atomic Gas, Science **336**, 887 (2012).

[24] E. H. Lieb and D. W. Robinson, The finite group velocity of quantum spin systems, Commun. Math. Phys. **28**, 251 (1972).

[25] Z.-X. Gong, M. Foss-Feig, S. Michalakis, and A. V. Gorshkov, Persistence of Locality in Systems with Power-Law Interactions, Phys. Rev. Lett. **113**, 030602 (2014).

[26] M. Foss-Feig, Z.-X. Gong, C. W. Clark, and A. V. Gorshkov, Nearly Linear Light Cones in Long-Range Interacting Quantum Systems, Phys. Rev. Lett. **114**, 157201 (2015).

[27] P. Hauke and L. Tagliacozzo, Spread of Correlations in Long-Range Interacting Quantum Systems, Phys. Rev. Lett. **111**, 207202 (2013).

[28] J. Schachenmayer, B. P. Lanyon, C. F. Roos, and A. J. Daley, Entanglement Growth in Quench Dynamics with Variable Range Interactions, Phys. Rev. X **3**, 031015 (2013).

[29] L. Vanderstraeten, M. Van Damme, H. P. Büchler, and F. Verstraete, Quasiparticles in Quantum Spin Chains with Long-Range Interactions, Phys. Rev. Lett. **121**, 090603 (2018).

[30] A. S. Buyskikh, M. Fagotti, J. Schachenmayer, F. Essler, and A. J. Daley, Entanglement growth and correlation spreading with variable-range interactions in spin and fermionic tunneling models, Phys. Rev. A **93**, 053620 (2016).

[31] M. B. Hastings and T. Koma, Spectral gap and exponential decay of correlations, Commun. Math. Phys. **265**, 781 (2006).

[32] M. F. Maghrebi, Z.-X. Gong, and A. V. Gorshkov, Continuous Symmetry Breaking in 1D Long-Range Interacting Quantum Systems, Phys. Rev. Lett. **119**, 023001 (2017).

[33] N. D. Mermin and H. Wagner, Absence of Ferromagnetism or Antiferromagnetism in One- or Two-Dimensional Isotropic Heisenberg Models, Phys. Rev. Lett. **17**, 1133 (1966).

[34] M. Kormos, M. Collura, G. Takács, and P. Calabrese, Real-time confinement following a quantum quench to a non-integrable model, Nat. Phys. **13**, 246 (2017).

[35] J. Greensite, An introduction to the confinement problem, Lect. Notes Phys. **821**, 1 (2011).

[36] N. Vandersickel and D. Zwanziger, The Gribov problem and QCD dynamics, Phys. Rep. **520**, 175 (2012).

[37] R. Coldea, D. A. Tennant, E. M. Wheeler, E. Wawrzynska, D. Prabhakaran, M. Telling, K. Habicht, P. Smeibidl, and K. Kiefer, Quantum Criticality in an Ising Chain: Experimental Evidence for Emergent E_8 Symmetry, Science **327**, 177 (2010).

[38] S. B. Rutkevich, Energy spectrum of bound-spinons in the quantum Ising spin-chain ferromagnet, J. Stat. Phys. **131**, 917 (2008).

[39] C. M. Morris, R. V. Aguilar, A. Ghosh, S. M. Koohpayeh, J. Krizan, R. J. Cava, O. Tchernyshyov, T. M. McQueen, and N. P. Armitage, Hierarchy of Bound States in the One-Dimensional Ferromagnetic Ising Chain $CoNb_2O_6$ Investigated by High-Resolution Time-Domain Terahertz Spectroscopy, Phys. Rev. Lett. **112**, 137403 (2014).

[40] J. A. Kjäll, F. Pollmann, and J. E. Moore, Bound states and E_8 symmetry effects in perturbed quantum Ising chains, Phys. Rev. B **83**, 020407 (2011).

[41] G. Delfino, Quantum quenches with integrable pre-quench dynamics, J. Phys. A **47**, 402001 (2014).

[42] G. Delfino and J. Viti, On the theory of quantum quenches in near-critical systems, J. Phys. A **50**, 084004 (2017).

[43] P. Calabrese, F. H. L. Essler, and M. Fagotti, Quantum Quench in the Transverse-Field Ising Chain, Phys. Rev. Lett. **106**, 227203 (2011).

[44] G. Delfino, Correlation spreading and properties of the quantum state in quench dynamics, Phys. Rev. E **97**, 062138 (2018).

[45] B. M. McCoy and T. T. Wu, Two-dimensional Ising field theory in a magnetic field: Breakup of the cut in the two-point function, Phys. Rev. D **18**, 1259 (1978).

[46] B. M. McCoy and T. T. Wu, Theory of a two-dimensional Ising model with random impurities. I. Thermodynamics, Phys. Rev. **176**, 631 (1968).

[47] B. M. McCoy and J.-M. Maillard, The importance of the Ising model, Prog. Theor. Phys. **127**, 791 (2012).

[48] M. C. Bañuls, J. I. Cirac, and M. B. Hastings, Strong and Weak Thermalization of Infinite Nonintegrable Quantum Systems, Phys. Rev. Lett. **106**, 050405 (2011).

[49] C.-J. Lin and O. I. Motrunich, Quasiparticle explanation of the weak-thermalization regime under quench in a non-integrable quantum spin chain, Phys. Rev. A **95**, 023621 (2017).

[50] J. Zhang, P. W. Hess, A. Kyprianidis, P. Becker, A. Lee, J. Smith, G. Pagano, I.-D. Potirniche, A. C. Potter, A. Vishwanath, N. Y. Yao, and C. Monroe, Observation of a discrete time crystal, Nature (London) **543**, 217 (2017).

[51] P. W. Hess, P. Becker, H. B. Kaplan, A. Kyprianidis, A. C. Lee, B. Neyenhuis, G. Pagano, P. Richerme, C. Senko, J. Smith, W. L. Tan, J. Zhang, and C. Monroe, Non-thermalization in trapped atomic ion spin chains, Phil. Trans. R. Soc. A **375**, 20170107 (2017).

[52] F. Machado, G. D. Meyer, D. V. Else, C. Nayak, and N. Y. Yao, Exponentially slow heating in short and long-range interacting floquet systems, arXiv:1708.01620.

[53] H. Bernien, S. Schwartz, A. Keesling, H. Levine, A. Omran, H. Pichler, S. Choi, A. S. Zibrov, M. Endres, M. Greiner, V. Vuletić, and M. D. Lukin, Probing many-body dynamics on a 51-atom quantum simulator, Nature (London) **551**, 579 (2017).

[54] S. Sachdev, *Quantum Phase Transitions* (Cambridge University Press, Cambridge, England, 2011).

[55] T. Koffel, M. Lewenstein, and L. Tagliacozzo, Entanglement Entropy for the Long-Range Ising Chain in a Transverse Field, Phys. Rev. Lett. **109**, 267203 (2012).

[56] M. Knap, A. Kantian, T. Giamarchi, I. Bloch, M. D. Lukin, and E. Demler, Probing Real-Space and Time-Resolved Correlation Functions with Many-Body Ramsey Interferometry, Phys. Rev. Lett. **111**, 147205 (2013).

[57] S. Fey and K. P. Schmidt, Critical behavior of quantum magnets with long-range interactions in the thermodynamic limit, Phys. Rev. B **94**, 075156 (2016).

[58] S. Fey, S. C. Kapfer, and K. P. Schmidt, Quantum Criticality of Two-Dimensional Quantum Magnets with Long-Range Interactions, Phys. Rev. Lett. **122**, 017203 (2019).

[59] P. Jurcevic, H. Shen, P. Hauke, C. Maier, T. Brydges, C. Hempel, B. P. Lanyon, M. Heyl, R. Blatt, and C. F. Roos, Direct Observation of Dynamical Quantum Phase Transitions in an Interacting Many-Body System, Phys. Rev. Lett. **119**, 080501 (2017).

[60] P. Calabrese and J. Cardy, Time Dependence of Correlation Functions Following a Quantum Quench, Phys. Rev. Lett. **96**, 136801 (2006).

[61] D. J. Luitz and Y. B. Lev, The ergodic side of the many-body localization transition, Ann. Phys. (Berlin) **529**, 1600350 (2017).

[62] A. Nauts and R. E. Wyatt, New Approach to Many-State Quantum Dynamics: The Recursive-Residue-Generation Method, Phys. Rev. Lett. **51**, 2238 (1983).

[63] See Supplemental Material at http://link.aps.org/supplemental/10.1103/PhysRevLett.122.150601 for detailed numerics of light-cone spreading of the correlations and discussions on convergent and scaling properties of mesonic masses.

[64] For Fig. 2(b), we use parameters and probing time relevant to current trapped-ion experiments [12,13,15].

[65] V. Zauner-Stauber and J. C. Halimeh, Probing the anomalous dynamical phase in long-range quantum spin chains through Fisher-zero lines, Phys. Rev. E **96**, 062118 (2017).

[66] J. C. Halimeh, V. Zauner-Stauber, I. P. McCulloch, I. de Vega, U. Schollwöck, and M. Kastner, Prethermalization and persistent order in the absence of a thermal phase transition, Phys. Rev. B **95**, 024302 (2017).

[67] J. C. Halimeh and V. Zauner-Stauber, Dynamical phase diagram of quantum spin chains with long-range interactions, Phys. Rev. B **96**, 134427 (2017).

[68] S. B. Rutkevich, On the weak confinement of kinks in the one-dimensional quantum ferromagnet $CoNb_2O_6$, J. Stat. Mech. (2010) P07015.

[69] The energy difference between (bounded) excited states at $k = 0$ and the ground state.

[70] E. C. Titchmarsh and D. R. Heath-Brown, *The Theory of the Riemann Zeta-Function* (Oxford University Press, Oxford, 1986).

[71] L. F. Santos, F. Borgonovi, and G. L. Celardo, Cooperative Shielding in Many-Body Systems with Long-Range Interaction, Phys. Rev. Lett. **116**, 250402 (2016).

[72] A. J. A. James, R. M. Konik, and N. J. Robinson, Nonthermal states arising from confinement in one and two dimensions, arXiv:1804.09990 [Phys. Rev. Lett. (to be published)].

[73] P. P. Mazza, G. Perfetto, A. Lerose, M. Collura, and A. Gambassi, Suppression of transport in non-disordered quantum spin chains due to confined excitations, arXiv:1806.09674.

[74] T. Rakovszky, M. Mestyán, M. Collura, M. Kormos, and G. Takács, Hamiltonian truncation approach to quenches in the Ising field theory, Nucl. Phys. **B911**, 805 (2016).

[75] N. J. Robinson, A. J. A. James, and R. M. Konik, Signatures of rare states and thermalization in a theory with confinement, arXiv:1808.10782.

[76] J. R. Garrison and T. Grover, Does a Single Eigenstate Encode the Full Hamiltonian?, Phys. Rev. X **8**, 021026 (2018).

[77] I.-D. Potirniche, A. C. Potter, M. Schleier-Smith, A. Vishwanath, and N. Y. Yao, Floquet Symmetry-Protected Topological Phases in Cold-Atom Systems, Phys. Rev. Lett. **119**, 123601 (2017).

[78] C. W. von Keyserlingk and S. L. Sondhi, Phase structure of one-dimensional interacting floquet systems. i. abelian symmetry-protected topological phases, Phys. Rev. B **93**, 245145 (2016).

[79] C. W. von Keyserlingk and S. L. Sondhi, Phase structure of one-dimensional interacting Floquet systems. II. Symmetry-broken phases, Phys. Rev. B **93**, 245146 (2016).

[80] A. C. Potter, T. Morimoto, and A. Vishwanath, Classification of Interacting Topological Floquet Phases in One Dimension, Phys. Rev. X **6**, 041001 (2016).

[81] D. V. Else and C. Nayak, Classification of topological phases in periodically driven interacting systems, Phys. Rev. B **93**, 201103 (2016).

[82] G. Delfino and P. Grinza, Confinement in the q-state Potts field theory, Nucl. Phys. **B791**, 265 (2008).

[83] L. Lepori, G. Z. Tóth, and G. Delfino, The particle spectrum of the three-state Potts field theory: A numerical study, J. Stat. Mech. (**2009**) P11007.

[84] S. B. Rutkevich, Baryon masses in the three-state Potts field theory in a weak magnetic field, J. Stat. Mech. (2015) P01010.

[85] M. Lencsés and G. Takács, Confinement in the q-state Potts model: An RG-TCSA study, J. High Energy Phys. 09 (2015) 146.